Barman Ishan (Orcid ID: 0000-0003-0800-0825)

Leveraging coffee ring effect on plasmonic paper substrate for sensitive analyte detection using Raman spectroscopy

Zufang Huang [a, b], Arun Nagpal [c], Soumik Siddhanta [a], Ishan Barman [a,d]

[a] Department of Mechanical Engineering, Johns Hopkins University, Baltimore, Maryland 21218, USA.

[b] Key Laboratory of OptoElectronic Science and Technology for Medicine of Ministry of Education, Fujian Provincial Key Laboratory of Photonics Technology, Fujian Normal University, Fuzhou 350007, P. R. China

[c] Department of Electrical Engineering, University of Michigan, Ann Arbor, Michigan 48109, USA

[d] Department of Oncology, Johns Hopkins School of Medicine, Baltimore, Maryland 21287, USA.

Abstract: Raman spectroscopy has demonstrated immense value as a molecular fingerprinting tool in biomedical diagnostics. However, the utility of conventional Raman scattering for ultrasensitive measurements of biofluids is limited by intrinsically weak signals, and has spurred advances in and wider applications of plasmon-enhanced measurements. Here, we propose a label-free methodology that leverages drop coating deposition on a silver ink-based plasmonic paper substrate with tunable hydrophobic attributes to combine two distinct sources of enhancement, namely solute pre-concentration and excitation of localized surface plasmons. The facile modulation of the hydrophobicity of the plasmonic silver paper facilitates investigations into the coffee-ring effect that results from the interplay of contact line pinning, solvent evaporation and capillary flow. We show that the Raman spectra acquired from the hydrated ring deposits show clear enhancement beyond that obtained from surface-enhancement owing to the presence of the silver nanofilm. In light of the superior sensitivity and lack of substantive sample preparation requirements, our findings open the door for a complementary low-cost paper-based analytical device for molecular sensing.

Owing to the wealth of vibrational mode information encoded in the spectral profiles, Raman spectroscopy offers the ability to probe biomolecular changes, and to detect complex molecular heterogeneity directly from biofluids, cells and tissues [1, 2]. Yet, its inherently weak signals make the approach unsuitable for direct measurements of <1 mM analyte concentrations, which in turn creates a major impediment for biomedical applications. To address the poor signal sensitivity, significant efforts have delved into the development of surface-enhanced Raman scattering (SERS) platforms that retain the exquisite molecular specificity and the innate immunity to photobleaching attributes of the spontaneous Raman measurements. SERS amplifies the Raman scattering signal obtained from the molecules adsorbed on or in close vicinity of noble metal nanostructures, which results in a strongly enhanced electric field due to the localized surface plasmon resonance (LSPR). In such environments, Raman signals, therefore, can be dramatically increased by several orders of magnitude to achieve high sensitivity detection of chemical and structural information of biomolecules[3]. The ability to reliably control the surface characteristics of the nanostructures has transformed SERS from an esoteric method to a robust analytical tool that is finding wider adoption in biochemical analysis and disease diagnosis[4,5].

Unlike the rigid SERS substrates generated using complex methods that often require sophisticated fabrication facilities[6], paper-based SERS substrates offer competitive advantages in terms of low cost of fabrication, inherent flexibility and simplicity[7], and sample conservation making it particularly favorable for on-site analytical analysis[8]. Conventionally, paper-based SERS substrates for Raman measurements

of bio-fluids has been achieved either through inkjet printing or colloidal nanoparticle soaking method, both of which have demonstrated highly sensitive detection. However, the soaking method is often time-consuming to achieve enough loading of nanoparticles while nanoparticles for printing need to be properly prepared into a suitable ink in order to be dispensed uniformly on the paper substrate and avoid potential clogging[9]. In addition, the random aggregation of nanoparticles, which are responsible for SERS performance on paper substrate through generation of "hot spots", can be challenging to control during the process of substrate preparation[6]. We have recently developed a complementary approach to the existing suite of fabrication techniques by simply heating the silver ink–fiber composite to achieve the formation of silver nanostructures entangled into the cellulosic substrate[10]. Specifically, our approach permits the engineering of distinct spatial domains with tunable wettability that ensures optimal analyte flow and, hence, better conditions for SERS measurements, as evidenced by the highly sensitive detection of P-selectin, a key diagnostic marker for heparin induced thrombocytopaenia.

Nevertheless, an outstanding challenge in harnessing plasmonic-based nanosensors for directly detecting molecules dissolved in dilute solutions is the difficulty in achieving satisfactory adsorption of analytes onto the hot spots. The diffusive natures of the analytes, which permit their motion far from the SERS-sensitive nanostructures, necessitates significant accumulation times (far beyond practical timescales) [11, 12] and has led to theorization of a "diffusion limit" in SERS analysis[13, 14]. Researchers have designed super-hydrophobic surfaces on silica wafer to overcome the diffusion limit of analytes in aqueous solutions. Additionally, in a recent study by Wong and co-workers, a slippery, omniphobic substrate, featuring glass slide as the base layer, that permits concentration of analytes and SERS substrates within an liquid droplet has been successfully used[13]. However, such approaches have not

been extended to plasmonic paper substrates. Traditional methods for fabrication of plasmonic paper substrate mostly form a hydrophilic surface, resulting in a vertical and horizontal capillary spreading through cellulose fibers once sample was loaded. This leads to the aforementioned reduction of the density of analytes on the substrate surface, which induces a decrease in detection sensitivity.

Here, building on these seminal studies on analyte pre-concentration, we reason that our silver ink precursor based synthesis approach can create plasmonic paper substrates with tunable hydrophobicity. In the pursuit of engineering such paper substrates with strong plasmonic enhancement, we observed the generation of the "coffee ring" that arises from analyte deposition within a drying drop as a result of the interplay of contact line pinning, solvent evaporation and capillary effects[15]. It is to be noted that the complex drying process is dictated by several effects such as the particle size, solvents and the droplet sizes, as detailed in the literature.[16-18] The coffee-ring effect enables the acquisition of Raman spectrum with high signal-to-noise ratio - importantly, without perturbing the secondary structure of the deposited proteins[19, 20]. Through the precursor-based fabrication of plasmonic paper, we propose and test a facile method that combines key features of drop coating deposition for sample pre-concentration and surface-enhanced Raman measurements. Given the advantages of label-free sensitive detection, quick data acquisition and low sample requirement, our method may offer a promising alternative for the development of health-relevant assays in resource-constrained settings as well as in addressing environmental monitoring platforms.

Fig. 1(A)-(C) illustrates the silver nanoink precursor-based preparation of the plasmonic paper substrate and the corresponding Raman measurements of the analytes deposited on the paper

substrate. As detailed in a recent article[10], the preparation of the plasmonic silver paper is a two-step process, namely coating the paper with ink followed by heating of the soaked paper. For coating of silver nanoparticles on paper substrate, Ag-ink stock solution was first prepared by adding isopropanol to the precursor (Kunshan Hisense Electronics Co., Ltd, China) and then sonicated for 10 min. Subsequently, the filter paper (Whatman grade 1) was soaked with Ag-ink solution for 15 min and then dried in the oven for 10 min at 130°C. In the former step, the ink solution is internalized and absorbed on the paper through the latter's wicking action. The wet film is decomposed on heating to yielding finely formed bare silver nanoparticles (see Fig. S1 in Supplementary Information). The use of a relatively low temperature and short heating time precludes extensive oxidation of the nanoparticles as well as degradation of the cellulosic substrate. In addition to generating distinct plasmonic attributes[10], tuning the ink concentration permits wettability transition to a hydrophobic regime owing to the nanoarchitecture of the resultant surface.

To examine the hydrophobicity of the silver nanoparticle embedded paper substrate, the contact angle was measured with a goniometer (Model 200, Ramé-Hart) using the sessile drop method [7]. **Table 1** details the contact angles measured as a function of the silver ink concentration used in the fabrication of the plasmonic paper substrate. Additionally, we tracked the time-dependent changes during the evaporation of micrometer-sized liquid droplets (**Fig. S2** in Supplementary Information). The hydrophobicity of the plasmonic silver paper arises due to the fine coating of silver nanoparticles on the cellulose strands of the filter paper. The nanoporous and fibrous structure of the substrate can potentially cause the water to penetrate in the cavities giving rise to adhesion. But in case of the plasmonic filter paper, the paper is completely covered with nanoparticles lowering adhesion. In case of

a substrate with nanoscopic roughness akin to the plasmonic substrate, the solid-liquid surface free energy of water is generally found to be higher, with the Cassie states arising from the reduction in number of interactions between the water and the solid surface.[21] We observed that the droplet evaporated with noticeable pinning at the contact line leading to a reduction of the contact angle over time, which in turn leads to the formation of the edge ring where the analyte is pre-concentrated.

To better visualize the formation of the coffee ring as a function of silver-ink: isopropanol concentration, 10 μL of 10^{-5} M rhodamine 6G (R6G) (Sigma Aldrich) solution was dropped and left to dry completely at room temperature. Fluorescence images were then obtained using the fluorescence stereo zoom microscope (Zeiss, Axio Zoom.V16), where the excitation and emission filters were set to 538-562 nm and 570-640 nm, respectively. **Fig. 2** illustrates a sharp fluorescence image of R6G deposition on Ag-ink paper substrate, showing a completely dark background outside the spot area. Higher fluorescence intensities were observed in the edge region than in the center from substrates treated with high Ag-ink concentrations (notably, 1:2 and 1:4 Ag ink: isopropanol volume ratio) that are consistent with drying patterns emanating from the capillary flow outwards to compensate for evaporative losses. A representative profile of fluorescence intensity along the radial direction of the dried spot on the 1:4 Ag-ink substrate (Fig. 2(a)) indicates that fluorescence intensity from the edge area is approximately two times greater than that recorded from the center region. One possible explanation for the phenomenon of moderate fluorescence existing inside the ring area is the absorption of the dye solution into the cellulosic fiber matrix during the slow solvent evaporation, even though the former process is considered slower than solvent evaporation[22].

However, for substrates treated with low silver-ink concentrations (such as, 1:16 and 1:32 silver-ink: isopropanol volume ratio), a more uniform (and brighter) fluorescence intensity distribution was observed. In addition to a reduced initial contact angle (**Table 1**), we observed less contact line pinning during solvent evaporation compared to the previous scenario for substrates treated with higher silver-ink concentrations. Furthermore, the brighter intensities may be attributed to the lesser quenching owing to the diminished nanoparticle density in these substrates. **Fig. 2(b)** confirms that higher edge-to-center intensity ratios were observed in substrates treated with higher concentrations of silver ink, whereas low concentrations of the same resulted in similar level of fluorescence intensity between the edge and center regions.

Next, to verify the presence of plasmonic enhancement of the deposited analytes on its surface, Raman measurements performed on the silver ink treated paper substrate and highly polished aluminum substrate were compared. Our choice of aluminum substrate as the control were governed by the high reflectivity and absence of Raman background, which makes it ideally suited for drop coating Raman measurements. 10μL of 10^{-5}M and 10^{-3}M R6G solution was dropped onto the plasmonic silver paper and aluminum substrates respectively, followed by complete drying at room temperature. Raman spectra were collected using a confocal Raman system (XploRA Plus, Horiba) equipped with a 514nm laser for excitation. The incident laser power was set to ~70μW and a 50x objective was employed to focus the excitation laser and collect the back-scattered signal. The exposure time was set to 2s and 3 successive frames were integrated. Raman spectra were collected (in triplicates) in the fingerprint range of 600-1800 cm^{-1}.

To assess the presence of drop coating pre-concentration based enhancement, we recorded SERS spectra from R6G solutions air dried on the plasmonic paper substrates. We observe that substrates treated with 1:4 and 1:8 silver-ink: isopropanol concentration show higher plasmonic enhancement, as evidenced by the more intense Raman profiles and the higher signal-to-noise ratios (**Fig. 3(A)**). In contrast, relatively modest spectral intensities (**Fig. 3(A)**) were observed from substrates treated with higher and lower silver ink concentrations (notably, 1:2 and 1:16 ink: isopropanol ratios). We reasoned that highly dense silver nanoparticles (for instance, obtained in the 1:2 silver ink treated substrate) coalesce, rather than aggregate, into larger structures that hinders hot-spot enhancement, whereas at low silver ink concentrations (e.g. in the 1:16 case), the paper surface is inadequately covered by the silver nanoparticles[10]. Importantly, the 1:4 and 1:8 substrates exhibit significantly higher edge-to-center Raman intensity ratio than the latter two (**Fig. 3(B)**). Clearly, the analyte pre-concentration in the characteristic coffee ring pattern plays a key role in the recorded spectral intensity. The observation of differences in strength of Raman peaks from the center and edge regions is also largely consistent with the prior findings from fluorescence imaging (**Fig. 2**), except for the slight discrepancy for the 1:2 silver ink treated substrate. The capillary flow that drags the analytes to the periphery is balanced by the absorption of analytes into the cellulosic matrix, which together determines the edge: center ratio of Raman signals observed. Hence, the silver-ink concentrations play a vital role in SERS enhancement as well as in determining distribution of the R6G molecules.

We also performed control measurements by drying a drop of the R6G solution on the aluminum substrate. Here, measurements in the center only revealed a broad fluorescence background, whereas Raman profiles with small peaks were observed from the edge area (**Fig. 3(C)**). The intensity of the

characteristic R6G peak (at 1649cm^{-1}) recorded from the 1:4 Ag-ink paper edge was approximately 10-fold larger than that acquired from the aluminum substrate, even though the concentration of R6G for the plasmonic paper measurements was two orders of magnitude lower than that employed in the aluminum substrate experiments.

It is worth noting that SERS is an extremely surface-selective process, i.e. sensitive to the distance between the nanoparticles and analytes being detected, which means that accumulation of large quantity of analytes in the annular ring does not guarantee uniform (or even strong) enhancement throughout its height. One can reasonably infer that the synergy of these two enhancement mechanisms occurs for a relatively thin layer of deposits, and the resultant spectral intensities do not benefit from both enhancements. The direct deposition of the analytes on the plasmonic paper substrate also plays a role in reproducibility of the signals. It presents an entirely complementary method compared to the ones where the liquid phase consists of mobile nanoparticles, the analyte molecules and the external aggregating agents, a combination of which may result in variable hot-spot formation.[23] The single component liquid phase in case of the plasmonic paper method makes the deposition process relatively independent of the variation of sample pH or other external factors, thus ensuring uniform enhancement from pre-formed hotspots.

It also follows that the signal enhancement is not necessarily linear with respect to analyte concentration. **Fig. 4(A)** plots the peak intensity at 1649cm^{-1} recorded from the 1:4 plasmonic silver paper as a function of R6G concentrations. Considerable deviation from a linear increase is observed and an eventual saturation phase is noted at *ca.* 10^{-4} M concentration when a large amount of R6G

molecules accumulated at the edge are out of the effective electromagnetic field enhancement region. Nevertheless, a low limit of detection is obtained for the plasmonic silver paper (LOD: 3.75×10^{-9} M), which combined with the high measurement reproducibility (low variations shown in **Fig. 4(A)**) makes this a promising platform for sensitive detection. By contrast, a much higher limit of detection and a wide-range linear relationship between the concentrations of analyte and the Raman intensity is noted when the measurements are performed on the aluminum substrate (**Fig. 4(B)**).

In summary, we report a facile method to realize drop coating deposition based pre-concentration of analytes and perform Raman measurements on a hydrophobic plasmonic paper substrate. Compared with the Raman spectra obtained from conventional DCDR substrates (such as aluminum), our plasmonic silver paper offers a much larger signal amplification stemming from two separate sources, namely the plasmonic enhancement and the analyte pre-concentration. Furthermore, our platform retains the benefits of other paper-based analytical devices including negligible fabrication cost (*ca.* 20 times cheaper than a plasmonic nanoparticle coated aluminum substrate), and ease of storage and transport that could potentially enable sensitive and label-free detection in biomedical, environmental and forensic applications. Our work also sheds light on the criticality of the silver ink coverage of the paper surface, which influences the plasmonic enhancement as well as the hydrophobicity and surface roughness-driven drying process. Our future studies will seek to test the feasibility of this technique to perform label-free multiplexed analyses by leveraging the ability to segregate different solutes based on their molecular weights and the exquisite specificity of the intrinsic Raman signatures.

Acknowledgement

References

1. Movasaghi Z, Rehman S, Rehman IU. Raman spectroscopy of biological tissues. *Applied Spectroscopy Reviews*. 2007; 42(5):493-541.

2. Butler HJ, Ashton L, Bird B, et al. Using Raman spectroscopy to characterize biological materials. *Nature protocols*. 2016; 11(4):664-687.

3. Kneipp K, Kneipp H, Bohr HG. Single-molecule SERS spectroscopy. In: *Surface-enhanced Raman scattering.* Springer; 2006; 261-277.

4. Tripp RA, Dluhy RA, Zhao Y. Novel nanostructures for SERS biosensing. *Nano Today*. 2008; 3(3):31-37.

5. Hering K, Cialla D, Ackermann K, et al. SERS: A versatile tool in chemical and biochemical diagnostics. *Analytical and bioanalytical chemistry*. 2008; 390(1):113-124.

6. Hoppmann EP, Wei WY, White IM. Inkjet-printed fluidic paper devices for chemical and biological analytics using surface enhanced Raman spectroscopy. *IEEE Journal of Selected Topics in Quantum Electronics*. 2014; 20(3):195-204.

7. Shao J, Tong L, Tang S, et al. PLLA nanofibrous paper-based plasmonic substrate with tailored hydrophilicity for focusing SERS detection. *ACS applied materials & interfaces*. 2015; 7(9):5391-5399.

8. Hoppmann EP, Wei WY, White IM. Highly sensitive and flexible inkjet printed SERS sensors on paper. *Methods*. 2013; 63(3):219-224.

9. Wei WY, White IM. Chromatographic separation and detection of target analytes from complex samples using inkjet printed SERS substrates. *Analyst*. 2013; 138(13):3679-3686.

10. Huang Z, Siddhanta S, Zhang C, Kickler T, Zheng G, Barman I. Painting and heating: A nonconventional, scalable route to sensitive biomolecular analysis with plasmon-enhanced spectroscopy. *J Raman Spectrosc*. 2017; 48(10):1365-1374.

11. Sheehan PE, Whitman LJ. Detection limits for nanoscale biosensors. *Nano letters*. 2005; 5(4):803-807.

12. Nair P, Alam M. Performance limits of nanobiosensors. *Appl Phys Lett*. 2006; 88(23):233120.

13. Yang S, Dai X, Stogin BB, Wong TS. Ultrasensitive surface-enhanced Raman scattering detection in common fluids. *Proc Natl Acad Sci USA*. 2016; 113(2):268-273.

14. De Angelis F, Gentile F, Mecarini F, et al. Breaking the diffusion limit with super-hydrophobic delivery of molecules to plasmonic nanofocusing SERS structures. *Nature Photonics*. 2011; 5(11):682-687.

15. Barman I, Dingari NC, Kang JW, Horowitz GL, Dasari RR, Feld MS. Raman spectroscopy-based sensitive and specific detection of glycated hemoglobin. *Anal Chem*. 2012; 84(5):2474-2482.

16. Yunker PJ, Still T, Lohr MA, Yodh AG. Suppression of the coffee-ring effect by shape-dependent capillary interactions. *Nature*. 2011; 476(7360):308-11.

17. Hu H, Larson RG. Marangoni effect reverses coffee-ring depositions. *J Phys Chem B.* 2006 ;110(14):7090-7094.

18. Shen X, Ho CM, Wong TS. Minimal size of coffee ring structure. *J Phys Chem B*. 2010; 114(16):5269-74.

19. Ortiz C, Zhang D, Xie Y, Ribbe AE, Ben-Amotz D. Validation of the drop coating deposition Raman method for protein analysis. *Anal Biochem*. 2006; 353(2):157-166.

20. Ganesh, Jeremy Peters Anna Luczak Varsha, Kalyanaraman EPR. Protein secondary structure determination using drop coat deposition confocal Raman spectroscopy. Spectroscopy. 2016; 31 (10): 31-39.

21. Leroy F, Müller-Plathe F. Rationalization of the Behavior of Solid– Liquid Surface Free Energy of Water in Cassie and Wenzel Wetting States on Rugged Solid Surfaces at the Nanometer Scale. *Langmuir*. 2010; 27(2):637-45.

22. Nilghaz A, Zhang L, Shen W. Coffee stains on paper. *Chemical Engineering Science*. 2015; 129:34-41.

23. Wang W, Yin Y, Tan Z, Liu J. Coffee-ring effect-based simultaneous SERS substrate fabrication and analyte enrichment for trace analysis. *Nanoscale.* 2014; 6(16):9588-93.
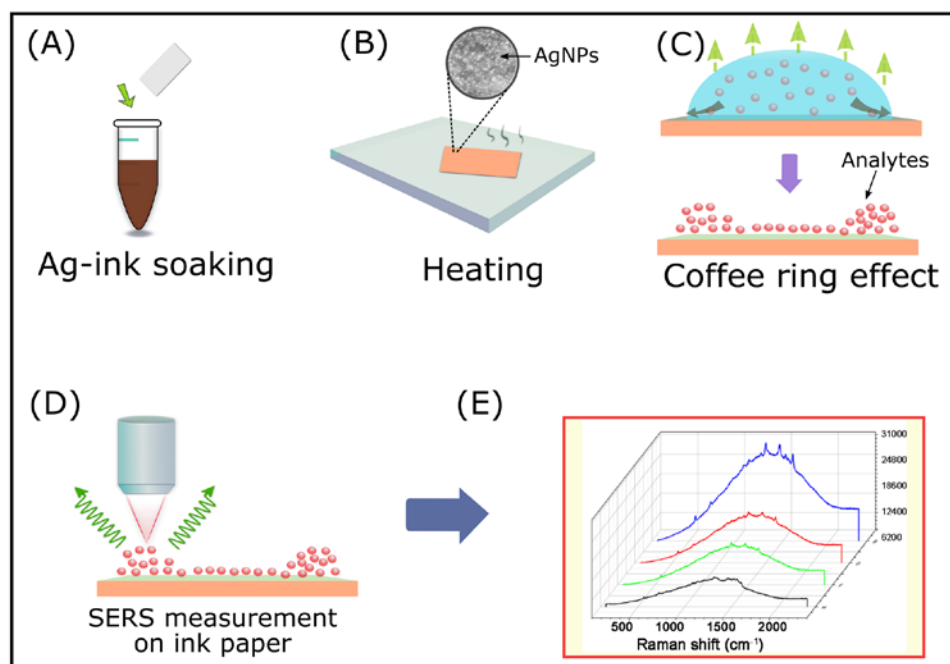
FIG. 1. Concept of drop coating deposition Raman measurements on plasmonic silver paper. (A)-(B) Schematic illustration showing the preparation of the plasmonic paper substrate using silver nanoink precursor. (C) Visualization of the analyte pre-concentration process on the plasmonic paper and formation of the coffee ring pattern owing to the hydrophobic nature of the substrate. (D) Acquisition of plasmon-enhanced Raman spectra from the approximate geometric center of the coffee ring, which are subsequently used to develop regression models to quantify the analytes of interest (E).
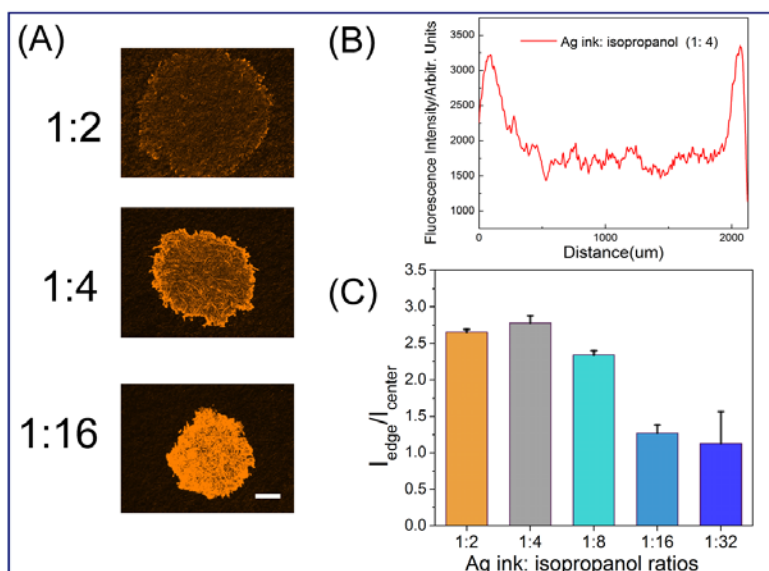
FIG. 2. (A) Representative fluorescence images of rhodamine6G (R6G) recorded on different silver-ink treated plasmonic paper substrates. The differential concentration of silver ink: isopropanol ratios used in preparing the substrate directly influences the hydrophobicity and, hence, the geometrical pattern of the deposits following droplet evaporation. Scale bar=500μm. (B) Fluorescence intensity profile along the radial direction, for the 1:4 silver ink: isopropanol treated paper, highlighting the formation of a "coffee ring" pattern of the R6G molecules. (C) Edge to center ratios of fluorescence intensity recorded from substrates treated with different concentrations of silver ink concentrations.
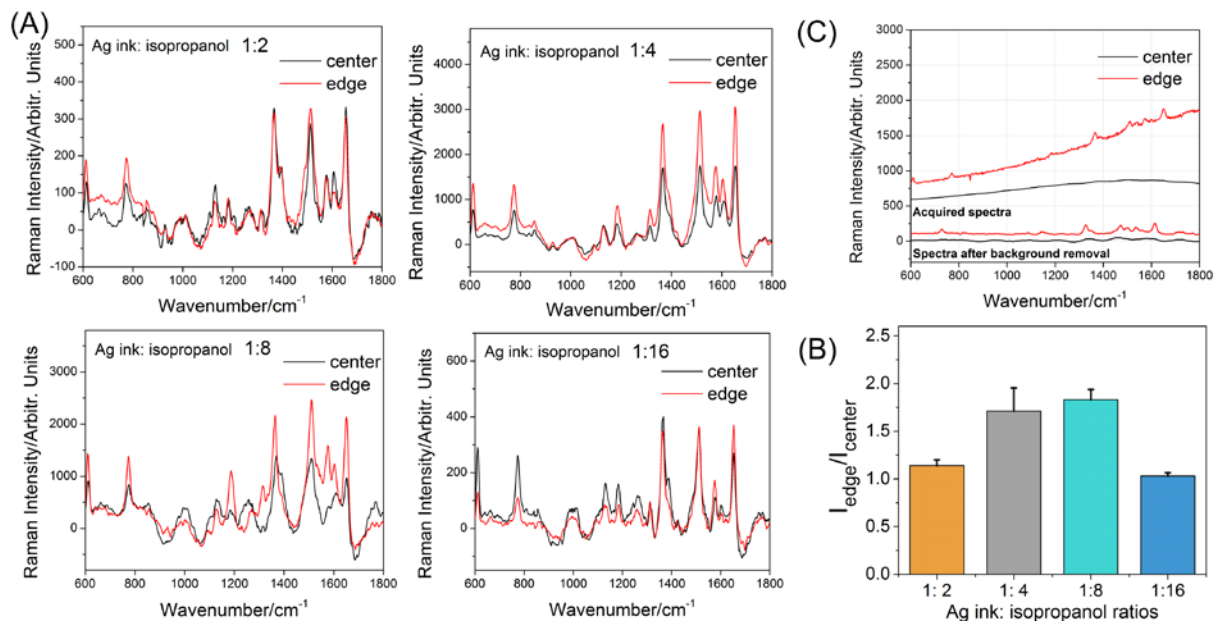
FIG. 3. (A) Representative Raman spectra acquired from R6G deposits in edge and center regions of paper substrates treated with varying silver-ink concentrations. (B) Edge to center ratios of Raman peak (at 1649 cm^{-1}) intensity recorded from substrates treated with different concentrations of silver ink concentrations. (C) Raman spectra acquired from edge and center regions of standard aluminum substrate, prior to and following fluorescence background subtraction.
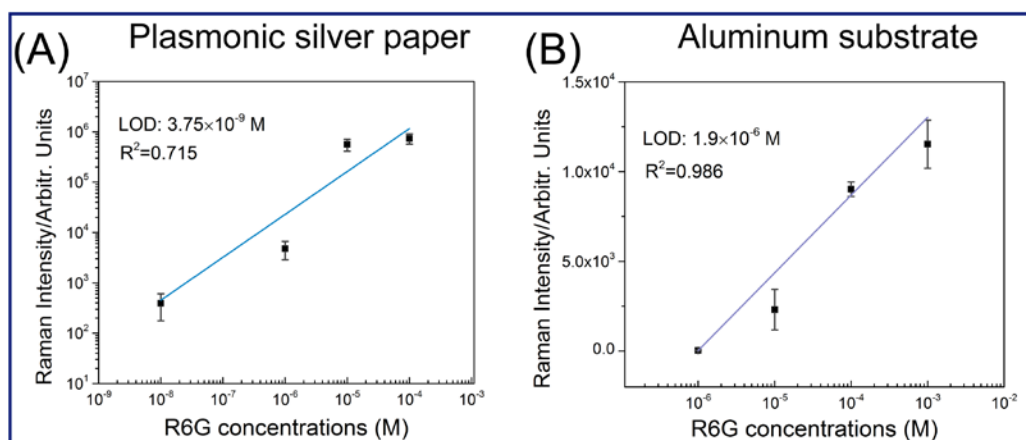

FIG. 4. Plots of intensity of Raman peak at 1649 cm^{-1} of R6G as a function of concentration recorded from: (A) plasmonic paper substrate treated with 1:4 silver ink: isopropanol ratio, and (B) aluminum

substrate. Spectra in each case were acquired immediately following air drying of the R6G solution pipetted on the substrate. The limits of detection and the coefficient of determination values are provided in the inset. The measurements were obtained in triplicates and the low standard deviation indicated by the error bars shows the excellent reproducibility of the plasmonic substrate.

Table 1. Water contact angle of plasmonic paper treated with different Ag-ink concentrations

Ink concentrations	Advancing contact angle	Receding contact angle	Contact angle hysteresis
1: 2	135.2±2.1	91.7±4.2	43.5±6.1
1: 4	132.4±3.4	89.9±1.9	42.5±5.0
1: 8	127.1±6.5	74.3±3.0	52.8±9.4
1: 16	120.3±5.5	74.0±1.2	45.4±5.0